SOILS AND FOUNDATIONS Vol. 34, No. 4, 33-41, Dec. 1994
Japanese Society of Soil Mechanics and Foundation Engineering

FAILURE MECHANISM IN GEOGRID-REINFORCED SEGMENTAL WALLS: EXPERIMENTAL IMPLICATIONS

DOV LESHCHINSKY[i], VICTOR KALIAKIN[ii], PARTHA BOSE[iii] and JAMES COLLIN[iv]

ABSTRACT

The results of pullout experiments employing one and two reinforcement layers are described. The results imply that the concept of an internal slip surface, passing through all reinforcement layers, may not always be valid. This validity is questioned when reinforcement layers, exhibiting significant stiffness at small strains, are closely spaced. The relevance of this observation to current design practice is also discussed.

Key words: geosynthetic, pullout resistance, reinforced soil, reinforced walls, slip surface (**IGC**: D10/E5/E12/H2).

INTRODUCTION

Current design guides for geosynthetically reinforced walls are based on limit state analysis (e.g., Leshchinsky and Perry, 1989; Jewell, 1990). In this analysis it is postulated that a slip surface will develop, extending between the toe and crest of the wall. The reinforcement must then extend beyond this slip surface so that lateral pressure against the facing of the wall is tied back (i.e., transferred) into the stable soil zone. Limit analysis, however, cannot account for the interaction between a system of alternating layers of geogrid and soil, and the subsequent possibility of load transfer or "shedding." If these layers are spaced far apart, one would expect little interaction, thus making the limit state design assumption sensible. However, as the spacing decreases, the geogrid-soil-geogrid interaction becomes stronger, producing a 'pseudo homogenized' structure that acts as an apparent monolithic block. Such a wall, comprised of the composite geogrid/soil, may be termed a 'Composite Wall.' This paper describes a preliminary experimental study, aimed at verifying if such a composite structure can be produced using available materials. It is tentatively concluded that the concept of an internal slip surface currently used in design, may not be valid when reinforcement layers, exhibiting significant stiffness at small strains, are closely spaced.

EXPERIMENTAL PROGRAM

Testing Plan

Two types of tests were conducted. The first type consisted of the pullout of a single geogrid layer. This was done to establish a performance baseline of the embedded geogrid under conventional test conditions. In addition, the testing facility and its potential end effects could be somewhat assessed by checking the single layer pullout test results for consistency. Also, the interaction coefficient characterizing the materials used, C_i, could be determined. Note that the interaction coefficient can be determined from a pullout test using:

$$T=2\cdot C_i\cdot\sigma\cdot L\cdot W\cdot\tan\phi \tag{1}$$

where T is the pullout force, C_i is the interaction coefficient, σ is the average stress normal to the geogrid plane, L and W are the length and width of the geogrid layer, respectively, and ϕ is the internal angle of friction.

The second type of test utilized two geogrid layers, attached to a rigid and smooth front panel, and pulled out through a force applied to this panel. This is a model test, and its relevance to current design is subsequently explained. The force versus displacement, as well as maximum pullout resistance from such tests can directly be compared with the single layer test results.

Pullout test conditions, for either the single layer or the double layer test, varied only with the confining pressure (i.e., induced normal stress) and the reinforcement

[i] Professor, Department of Civil Engineering, University of Delaware, Newark, Delaware 19716, USA.
[ii] Assistant Professor, ditto.
[iii] Formerly Graduate Student, ditto.
[iv] Vice President-Technology Development, Tensar Earth Technologies, Inc., 5775 B Glenridge Dr., Lake Side Center, Atlanta, Georgia 30328, USA.
Manuscript was received for review on January 11, 1994.
Written discussions on this paper should be submitted before July 1, 1995 to the Japanese Society of Soil Mechanics and Foundation Engineering, Sugayama Bldg. 4 F, Kanda Awaji-cho 2-23, Chiyoda-ku, Tokyo 101, Japan. Upon request the closing date may be extended one month.

length. A detailed description of the equipment, materials and test setup is presented below.

Testing Facilities

Figures 1 and 2 illustrate schematically the setup for the single and double layer pullout tests, respectively. A metal frame, 20 cm wide, was designed and constructed to carry out the pullout tests. For the single layer, the front end of the frame had a slot at its mid-height, through which the embedded geogrid was pulled (Fig. 1). In the double layer case, the two geogrids were attached to a 20 cm high panel that was subsequently subjected to a pullout load (Fig. 2). To minimize friction with soil, the panel was coated with grease and covered with a latex sheet. Two 1.9 cm thick transparent plexiglas panels made up the side walls of the testing box. The geogrid width, in all experiments, fitted exactly the inside net box width of $W=19$ cm. Movement of soil adjacent to the displacing geogrid could thus be observed through the transparent plexiglas walls. Channel sections were bolted at two intermediate levels on both outer sides of the pullout box to add lateral stiffness by restricting the relatively flexible plexiglas from bulging.

Confining pressure was applied at the top of the box through a custom-made air bag, capable of sustaining 207 kPa. Pullout force was applied using a Duff-Norton Screw Jactuator having a 56:1 gear ratio. A speed controlled electric motor powered the screw jack at a rate of approximately 0.25 cm per minute.

The pullout load was transferred through a load cell to two sheet metal plates in the single layer test (Fig. 1), or to the rigid facing panel in the double layer test (Fig. 2). The sheet metal plates in the single layer tests were 12.7 cm long and were attached to each other using epoxy, firmly and rigidly "sandwiching" the front end of the geogrid specimen 10 cm into the sand. This reduced the boundary effects at the front end of the testing box, while transmitting a uniform tensile load to the specimen. A similar technique was used in the double grid tests to firmly attach the two geogrids to the facing panel; the thickness of these sheet metal plates was equal to the facing thickness; i.e., about 5 cm. This assured uniform connection between the facing and the geogrids.

Displacements along the geogrids were measured using tell-tale connections to dial gages. In the single layer pullout test, three points along the specimen were monitored for displacement. In the double layer case, the common front end of the grids and both free ends were monitored. In all tests, movement of the free end indicated that pullout had occurred.

Materials

The soil used in all tests was dry Ottawa sand. The sand was densified to an average unit weight of 16.8 kN/m^3 ($D_r=70\%$). To achieve a near uniform unit weight, six layers of sand were placed in the box, each through sand 'raining.' A slight tapping on the box sides and on top of the sand, was sufficient to attain the prescribed unit weight of each layer placed. Triaxial tests, conducted on this sand at $D_r=70\%$ and at confining pressures varying between 69 and 207 kPa, gave ϕ_{peak} and $\phi_{residual}$ values of 38° and 34°, respectively. Typical grain size distribution of this poorly graded sand (*SP*) was $D_{90}=0.60$ mm, $D_{80}=0.42$ mm, $D_{60}=0.31$ mm, $D_{50}=0.26$ mm, $D_{30}=0.18$ mm, and $D_{10}=0.13$ mm. Maximum grain size was 0.90 mm.

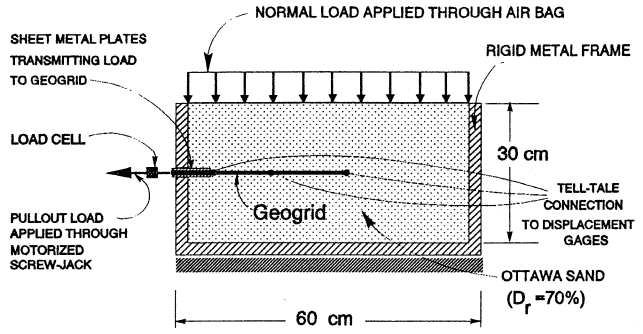

Fig. 1. Schematics of test setup: Single layer

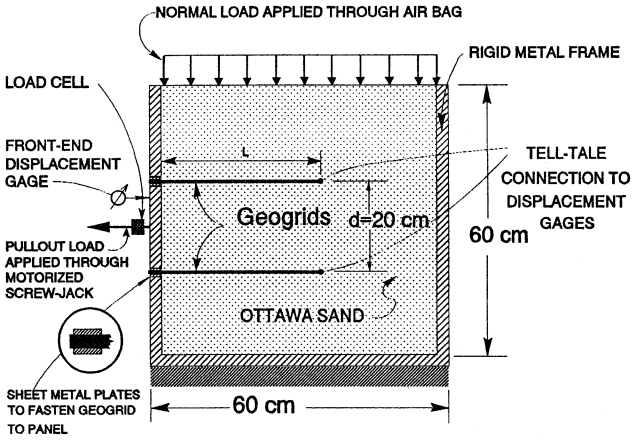

Fig. 2. Schematics of test setup: Double layer

The geogrid used was Tensar BX1500 made of Polypropylene. The tensile test results for this bi-axial geogrid, using the wide-width test method (ASTM D4595), are shown in Fig. 3. Its tensile strengths are 45.2 and 35.0 kN/m in the transverse and machine directions, respectively. All pullout tests were conducted with loading applied in the transverse direction. It should be pointed out that the wide-width test is carried out at a temperature of 21±2°C. Tensile load is applied so as to produce an average geogrid strain of 10% per minute. Time-dependent behavior of similar geogrids has been widely reported in the literature (e.g., McGown et al., 1984). Note, however, that little creep data is available for in-soil conditions.

Net aperture inside dimensions of the geogrid were 30.5 mm and 25.4 mm in the transverse and machine directions, respectively. The geogrid open area was 65%. Its thickness at the rib and junction was 1.8 mm and 4.8 mm, respectively. Its junction strength was 30.6 kN/m.

Latex sheets, 0.4 mm thick, were placed between each of the two transparent plexiglas side walls and the sand.

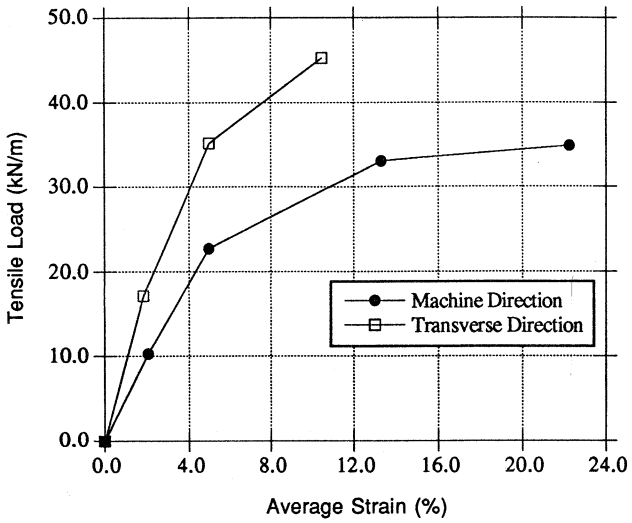

Fig. 3. Load-elongation curves for tensar BX1500 geogrid

The latex sheets were labeled with permanent markers to form a mesh of points. High quality silicone grease, manufactured by Shin-Etsu Chemical Company, was smeared on the latex sheets (on the side facing the transparent wall), as well as on the plexiglas walls. The nearly uniform thickness of the grease was about 0.1 mm. The grease allowed the latex sheets to be pasted to the side walls before sand was rained in. More importantly, this grease has extremely low adhesion, thus creating shear-free boundaries that allow the latex to deform with the sand while minimizing end-effects. In light of the fact that the box net inside width was only 19 cm, this is indeed an important consideration. The latex was thus assumed to move with the sand, and to depict the displacement field produced by the geogrid as it was subjected to gradually increasing pullout forces. The coordinates of the deforming mesh, marked on the latex, were later measured from photographs taken at various times in the loading history. The coordinate measurements utilized a digitizer connected to a PC. Hence, the displacement field within the sand, due to a given load increment, could be calculated with an accuracy better than 0.5 mm.

Scope of Tests

Nine pullout tests of the single layer were conducted. Three different grid lengths were used (17.15, 31.12 and 45.72 cm). The 17.15 cm long specimens were subjected to confining pressures of 69.0, 103.5 and 138 kPa; the 31.12 cm specimens were tested under 34.5, 69.0 and 103.5 kPa; and the 45.72 cm ones were subjected to 12.25, 41.4 and 69.0 kPa. Six pullout tests of the double layer were conducted for two lengths, 31.12 and 45.72 cm. The 31.12 cm long specimens were tested under confining pressures of 34.5, 69.0 and 103.5 kPa, while the 45.72 cm ones under 17.25, 34.5 and 69.0 kPa. All tests were planned such that pullout rather than breakage of geogrid would occur first.

TEST RESULTS

Figure 4 presents a summary of all single layer test results considering the *measured peak* pullout load. Rather than displaying pullout force, however, the average shear stress, defined as the *corrected* pullout load divided by twice the area of the specimen ($A=L\cdot W$ where A, L, and W are the area, length and width, respectively; i.e., the specimen is considered as a continuous sheet), is presented versus the applied normal stress. The corrected pullout load is the measured peak value minus friction loss due to the embedded sheet metal plate (see Fig. 1). This loss was determined from simulated pullout tests on embedded metal plates having the same dimensions as those used in the regular tests but without a geogrid attached. These calibration tests correlated the frictional loss, confining pressure and displacement, while assuming the plate to be rigid. Figure 4 implies that a straight line envelope is appropriate for all single layer test results. This line is inclined at about 29°. Hence, considering the peak value of both the internal angle of friction ($\phi_{peak}=38°$) and the pullout load, the interaction coefficient is about $C_i=0.71$. Figure 5 is similar to Fig. 4, but corresponds to the *measured residual* pullout load. The envelope here is inclined at about 25°, implying $C_i=0.69$ (recall: $\phi_{residual}=34°$). It should be pointed out that Figs. 10 through 15 show the peak pullout loads; *measured residual* pullout loads were observed at very large displacements (i.e., at about 50 mm). That is, though it is apparent from the figures that the displayed post-peak data has not reached yet its residual values in some cases (i.e., Figs. 10, 12, 14), the actual tests were continued until residual strength values were obtained. The recording of displacements ceased since the full range of the measuring device had been exceeded. However, the pullout load was recorded at constant time intervals to obtain the residual strength. In Fig. 10 the displacement device was not reset at the beginning of the test and therefore, its effective measurement range was

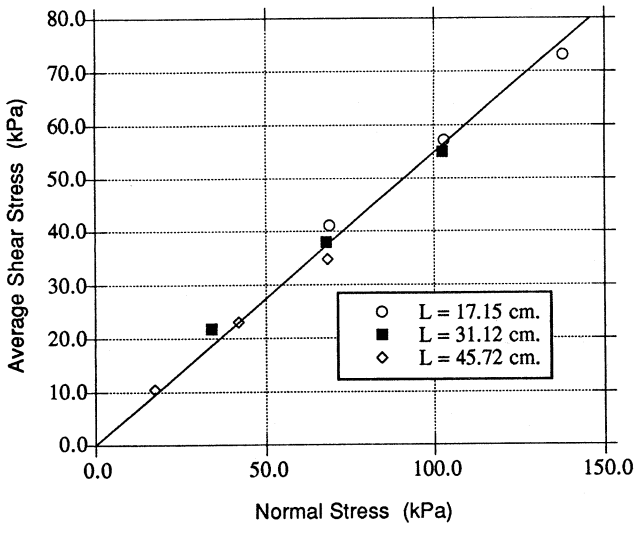

Fig. 4. Summary of single layer pullout test results: Peak values

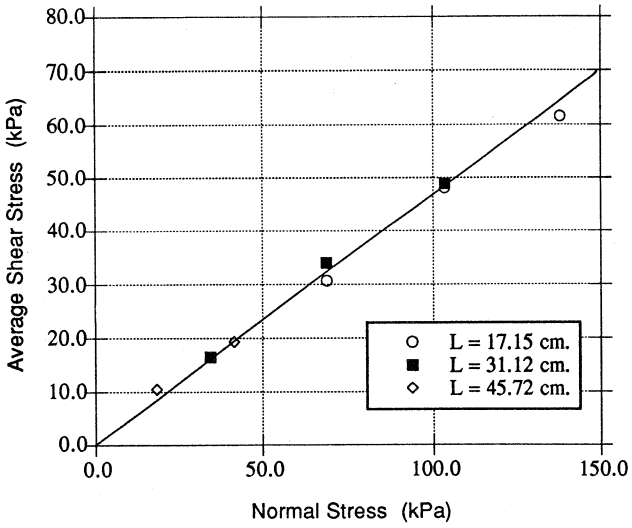

Fig. 5. Summary of single layer pullout test results: Residual values

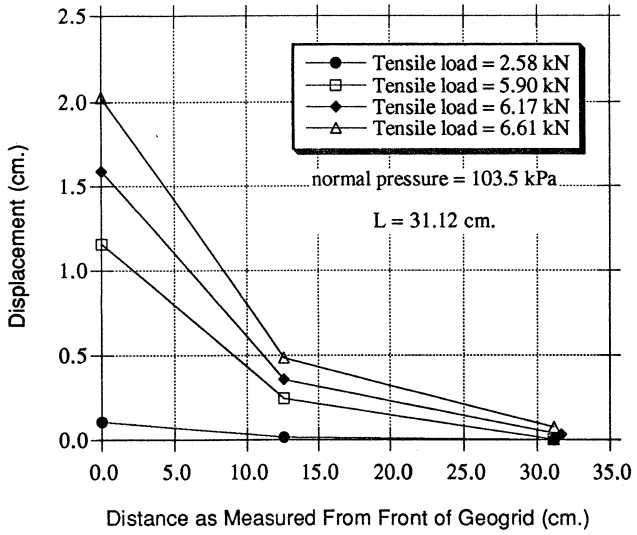

Fig. 6. Typical displacements along a geogrid at various pullout loads

limited to about 25 mm. The summary of test data in Fig. 5 corresponds to the actual residual values.

It should be pointed out that the process of pullout is a progressive phenomenon. That is, while a segment of the embedded geogrid is strained past the peak soil restraining capacity, portions away from the applied tensile load are hardly displaced (e.g., see Fig. 6 to realize how nonuniform the displacement along a geogrid is under tension). Hence, pullout does not occur simultaneously along the geogrid, as portions of its interface are already at their residual state. Consequently, for design it may be wise to use the residual pullout resistance. The test results indicate, however, that C_i associated with peak or residual values is practically the same. However, this conclusion is limited to Ottawa sand at $D_r = 70\%$; generally, this is not the case. Also, the value of C_i is somewhat small, though considering the consistency of the particles of Ottawa sand, this is not surprising.

Based on the results of single layer experiments, it appears that during pullout, 2.5 to 5 cm of soil on either side of the geogrid are affected. This observation is independent of the confining pressure. Figure 7 shows schematically a typical pattern of displacement observed in the sand. This displacement was the result of both rigid-body movement and deformation. With a realistic backfill, the influence zone will likely be larger. It should be noted, though, that in the majority of the single layer pullout tests the measured displacement field did not seem to accurately reflect the actual soil displacement. Hence, only qualitative observations (see Fig. 7) with regard to the displacement field can be made. That is, photogrammetric measurements of the latex mesh for the single layer pullout tests were deemed inaccurate.

Figures 8 and 9 show the pullout load versus the front-end displacement for all double layer tests. Note that the front-end displacement required to attain maximum pullout resistance increases with increase of confinement pressure or increase of embedded length of the geogrid. That is, when maximum pullout force is attained, larger

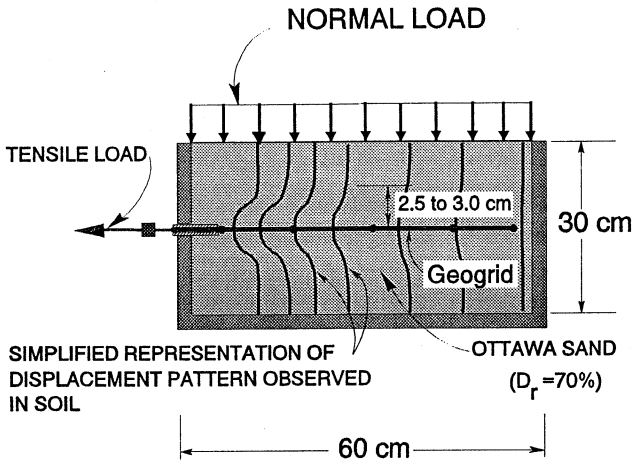

Fig. 7. Observed pattern of soil displacement as the geogrid is being pulled out

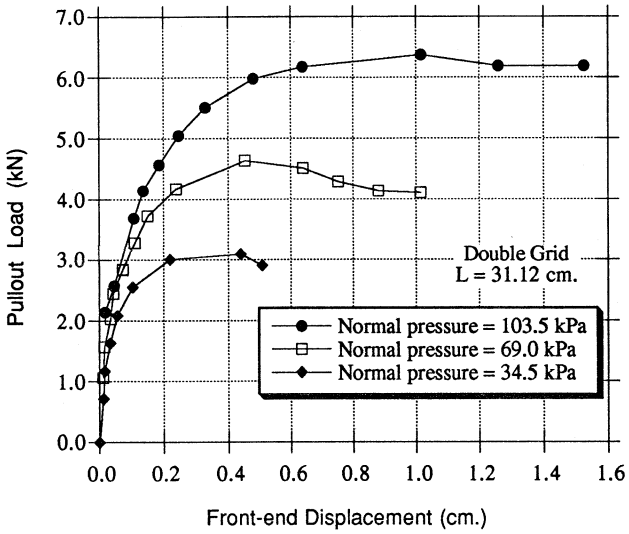

Fig. 8. Pullout test results for double layer ($L = 31.12$ cm.)

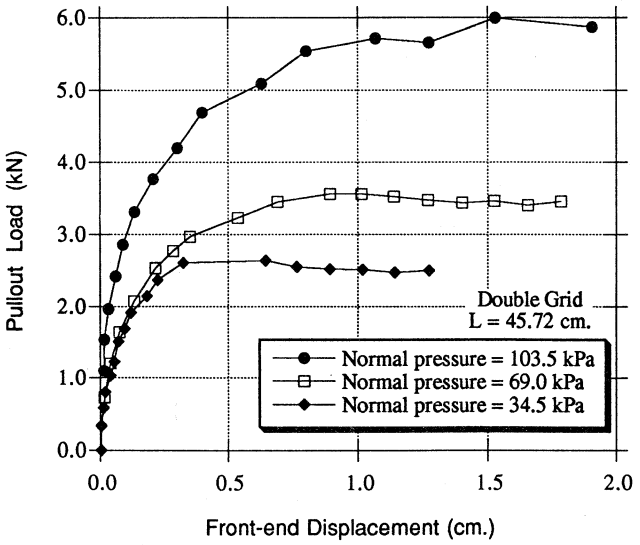

Fig. 9. Pullout test results for double layer (L=45.72 cm.)

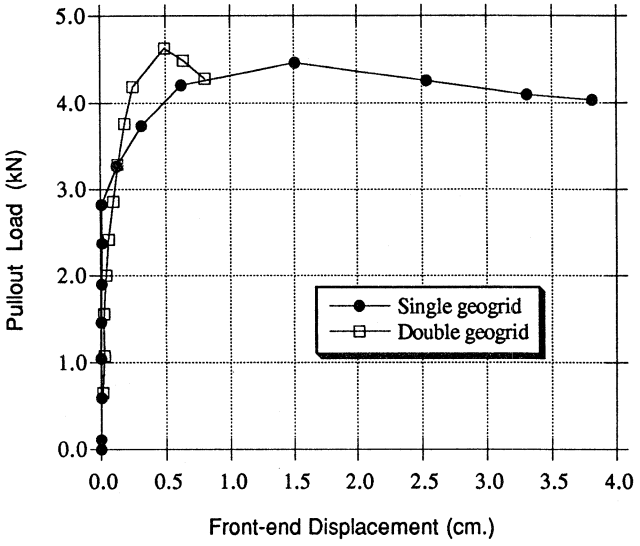

Fig. 11. Comparison of pullout curves: Single vs. double layer (L=31.12 cm.; σ=69.0 kPa)

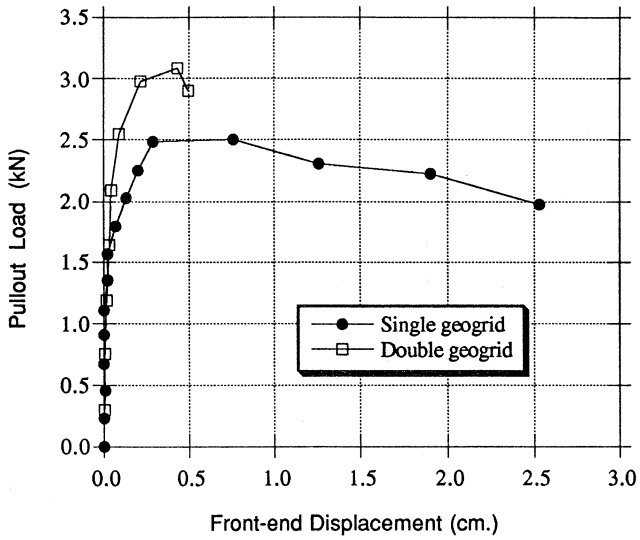

Fig. 10. Comparison of pullout curves: Single vs. double layer (L=31.12 cm.; σ=34.5 kPa)

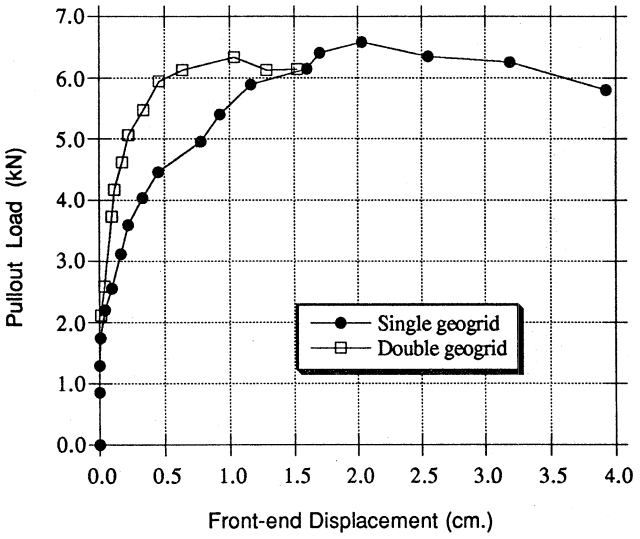

Fig. 12. Comparison of pullout curves: Single vs. double layer (L=31.12 cm.; σ=103.5 kPa)

strains are generated in the geogrid as the confining pressure or embedded length increases.

Figures 10 through 15 compare the single and double layer pullout load versus displacement curves, each for the same geogrid length. From these figures it is apparent that: 1) For higher confining pressures the maximum pullout resistance is nearly the same for single and double layers; however, for pressures less than 34.5 kPa, the double layer pullout appears to be as much as 30% larger; and 2) The front-end displacement associated with the double layer maximum pullout force is much smaller than that required for the single layer. Both observations imply that for overburden pressures likely in a typical wall structure, the material confined in between the two grids is stiffened, resulting in a nearly "rigid body" movement of the soil and reinforcement as a block. This block has the same surface area as the equivalent single layer grid and therefore, no significant increase in pullout resistance occurs when two layers are considered. Furthermore, when this block is subjected to pullout load, it undergoes very little internal deformation as compared to the progressive straining associated with the single layer. This results in small front-end displacements prior to pullout. In fact, the observed soil displacement field, schematically illustrated in Fig. 16, implies that the soil in between the geogrids indeed displaces as a block. A slide/pullout pattern was observed above the top layer, below the lower layer, and near the back-end of the geogrids.

Figure 17, similar to Fig. 4, summarizes all single and double layer test results corresponding to maximum pullout resistance. Generally, the single layer results agree with the double layer results when treating the double

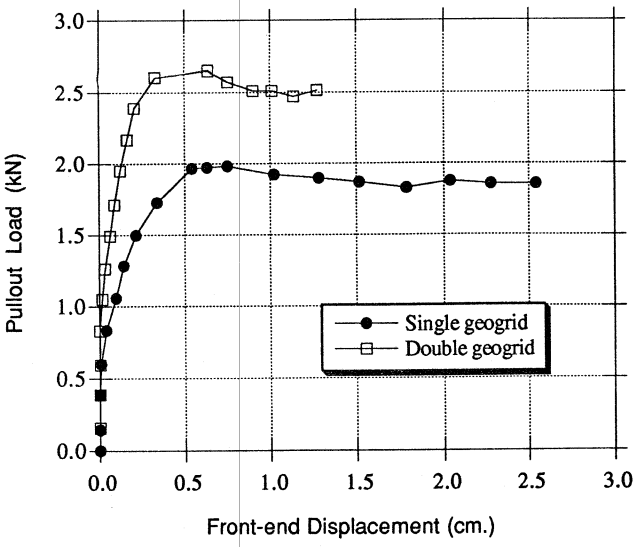

Fig. 13. Comparison of pullout curves: Single vs. double layer (L=45.72 cm.; σ=17.25 kPa)

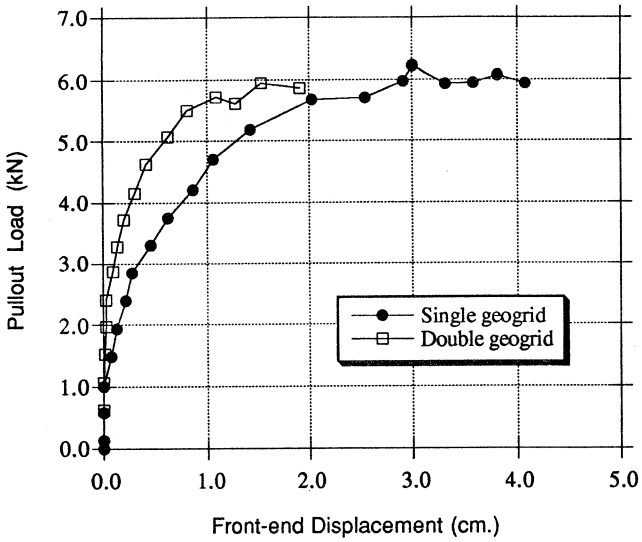

Fig. 15. Comparison of pullout curves: Single vs. double layer (L=45.72 cm.; σ=69.0 kPa)

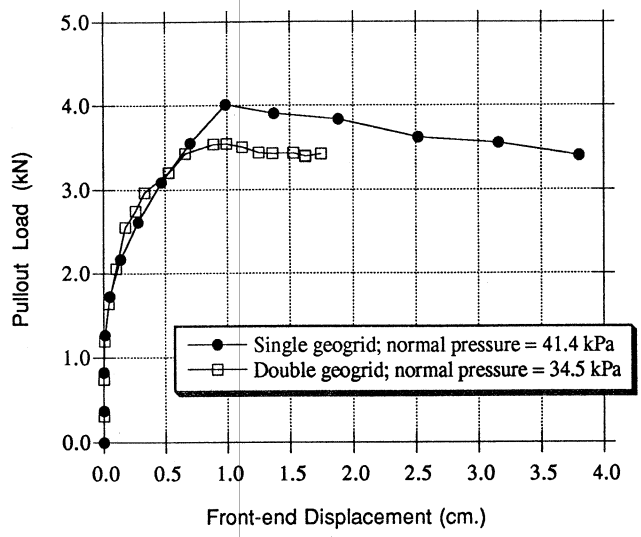

Fig. 14. Comparison of pullout curves: Single vs. double layer (L=45.72 cm.; σ=34.5 or 41.4 kPa)

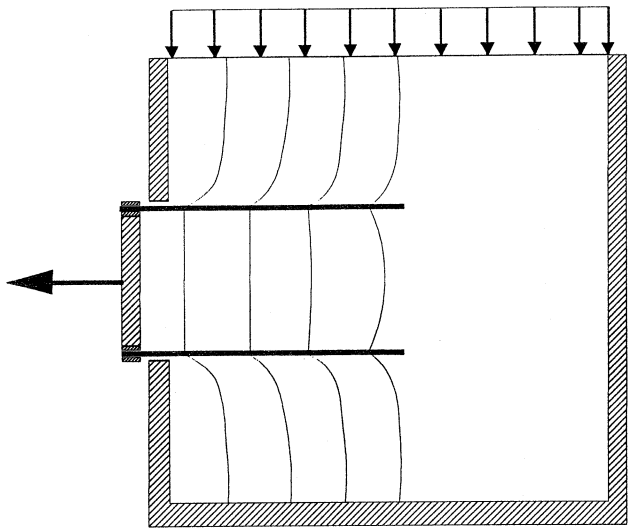

Fig. 16. Simplified representation of soil displacement pattern: Double layer movement

layer as a rigid block. Note, however, that for a double layer length of 31.12 cm, the average pullout stress is somewhat larger than for a length of 45.72 cm. A reasonable explanation for this phenomenon can be drawn from Fig. 16. That is, near the back-end a pullout mechanism of two geogrids prevails rather then the mechanism of a single block. This local pullout increases the overall pullout resistance; however, as the length of the block increases (say, from 31.12 to 45.72 cm), the overall effect of this local pullout contribution diminishes.

Figures 18 through 20 represent typical displacement fields measured in the double layer tests when pullout occurred. Note that there are two zones, above and below the double geogrids, where displacement was not measured. This was due to the metal channels, reinforcing and stiffening the testing box, that obstructed locally the view of the latex sheet. Also note that displacements at the lower portion of the box were negligible while vertical and horizontal displacements were noticeable in the upper portion above the geogrids. This is due to the different boundary conditions at the top and bottom of the box. The sketch in Fig. 16 is a simplified representation of these and other figures. Calculations of shear strains in the soil based on the displacement fields indicated very small strains, all below about 1%.

RELEVANCE OF TESTS TO CURRENT DESIGN PRACTICE

Current design methods for reinforced walls are based on a limit state approach; i.e., Rankine's or limit equilibrium (e.g., Coulomb's, log spiral, etc.). Basically, a slip surface is assumed to develop within the backfill,

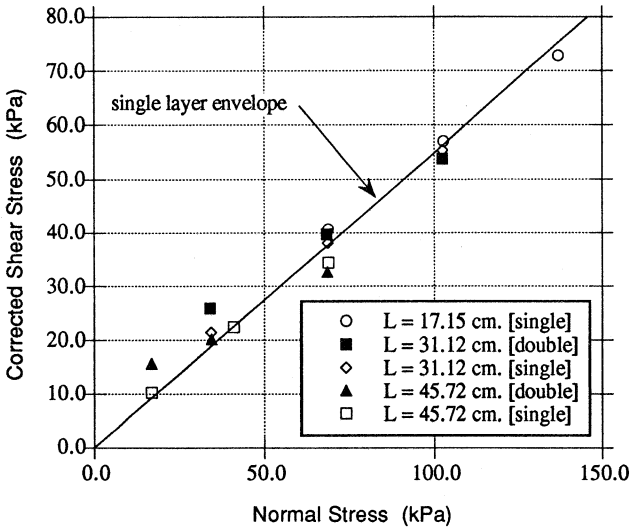

Fig. 17. Summary of peak pullout loads: Single and double layer tests

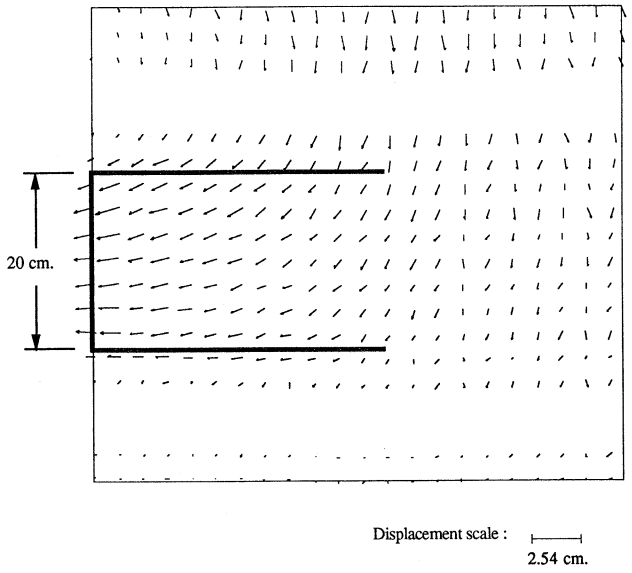

Fig. 18. Measured displacement field ($L=31.12$ cm., $\sigma=69.0$ kPa)

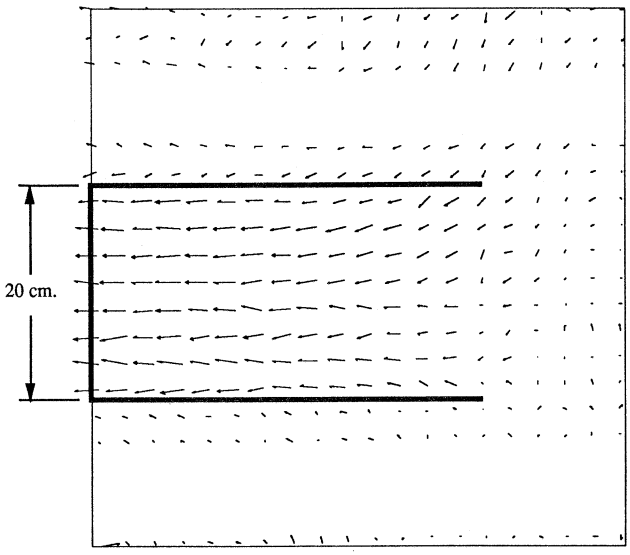

Fig. 19. Measured displacement field ($L=45.72$ cm., $\sigma=17.15$ kPa)

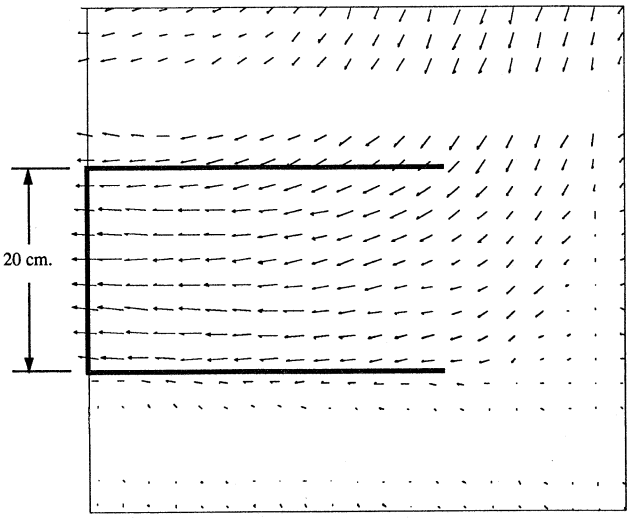

Fig. 20. Measured displacement field ($L=45.72$ cm., $\sigma=69.0$ kPa)

and to pass through the reinforcing layers. That is, an active soil wedge is formed within the reinforced zone. This wedge leans against the wall face. The resulting lateral load exerted against the facing units is transmitted back by the geogrid layers into the stable soil behind the active wedge. Based on the aforementioned postulated mechanism, a stable system is produced in which the geogrid layers act as tiebacks. Verification of the postulated mechanism is difficult to achieve in a framework of full scale tests. However, a model test consisting of one facing unit tied back by two geogrid layers and subjected to a predetermined simulated overburden pressure (i.e., confining pressure) can be conducted in a detailed fashion and with relative ease. In this model test, the outward movement of the single facing unit can be accurately and actively induced. Subsequent displacement within the soil can be observed to see if indeed a wedge has formed. The double layer pullout test is indeed this model test. Though in the actual structure outward movement will result from excessive overburden pressure, the simulation using induced facial displacement, while holding the confining pressure constant, is considered equivalent as far as the resulting failure is concerned. In a sense, this is analogous to failure in a triaxial specimen either through increase of σ_1 while holding σ_3 constant, or through decrease of σ_3 while σ_1 is held constant; the end result is the same inclination of the failure surface at an

angle of $(45° + \phi/2)$ to σ_3. Figure 21 shows the postulated initial failure mechanism used in current design methods as applied to the single facing unit. That is, as the facing unit is pulled outward, an active wedge is expected to form through the top geogrid layer. This wedge is to be restrained by the facing. As the facing (and the connected geogrids) is continuously pulled, the soil mass in between the two geogrids is expected to move together with the progressively straining geogrids. This causes the initially developed failure zone, which extends up to the soil surface, to shift to the right. The ultimate situation occurs when the pullout resistance is exceeded, provided the tensile force is smaller than the reinforcement break strength. The initial formation of an active wedge is considered as the failure state in design. In a wall structure, where facing units are stacked, active wedges (e.g., Rankine's) will emanate from the toe of each unit to the crest. In the model test, the formation of only one such wedge can be examined.

Contrary to the postulated mechanism used in current design of reinforced walls (Fig. 21), the mechanism shown in Fig. 22 was observed. That is, at 20 cm spacing an initial active wedge against the facing was not observed. Rather, the soil mass confined in between the two geogrids moved nearly as a rigid block. This movement occurred rapidly, after very little displacement of the facing (2 to 4 times smaller displacement than that associated with the pullout of an equivalent single geogrid). As the movement evolved, a wedge *behind* the two geogrids formed, similar to the one shown schematically in Fig. 22. This wedge represents a soil mass in an active state, retained by the composite geogrid-confined soil system.

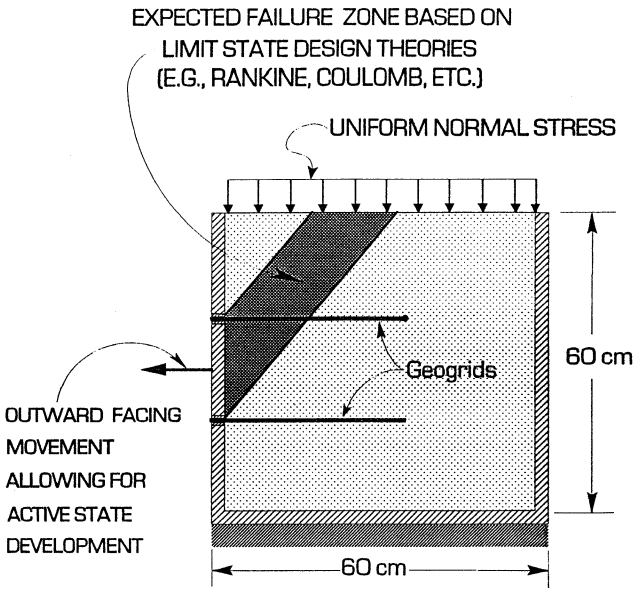

Fig. 21. Postulated initial failure mechanism in current design

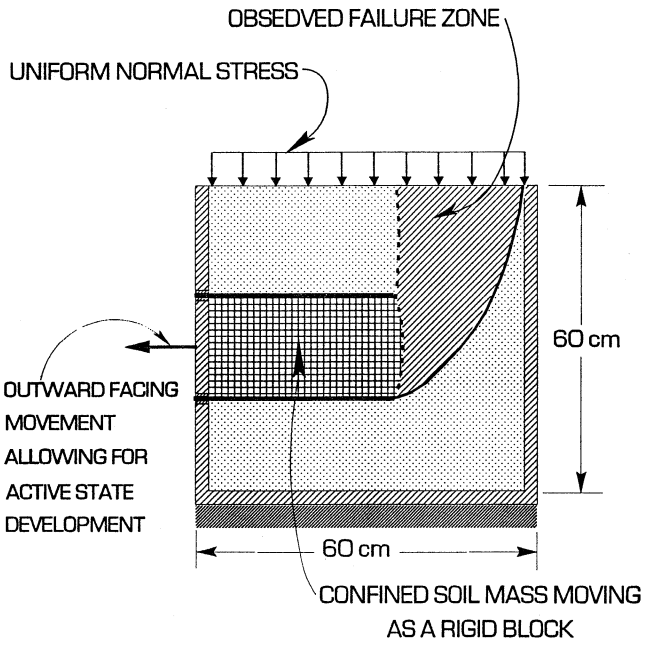

Fig. 22. Observed failure mechanism

CONCLUSIONS

Actual segmental walls include many geogrid layers that are attached to stacked facial units. The double layer pullout model test signifies one facial unit in such a wall, where failure is induced through lateral movement rather than through an increase in wall's height (i.e., increase in overburden, or confining, pressure). In either process, current design procedures assume the formation of an active wedge against the wall. However, with regard to these design procedures for reinforced segmental walls, the experimental observations noted herein imply the following:

1. If the reinforcement layers are closely spaced and are sufficiently stiff and strong, a failure surface entirely within the reinforced zone is *not* likely to develop. At a limit state, an active zone is likely to develop behind the reinforced zone.
2. The soil confined between the closely spaced geogrids is stiffened, forming a composite material that behaves, for simplified design purposes, as a monolithic block. Consequently, if all layers are of equal length and spacing, the reinforced backfill can be treated in design as a gravity wall. In this case, for granular backfill the length of the reinforcement can be as short as 0.3 to 0.4 times the height of the wall. This range stems from external stability considerations for a wall over competent foundation (i.e., direct sliding and overturning analyses), and it is considerably shorter than the range required based on a tieback wedge (0.6 to 0.7 times the height).
3. This pseudo gravity wall must retain an unreinforced soil mass behind it. This mass is in an active state, as is the soil behind the double layer (Fig. 22). Since the interface between the reinforced and unreinforced zones consists of soil (and not, say, concrete and soil), the force exerted by the active wedge may be assumed to be inclined at ϕ. This inclination is commonly used in design when utilizing a two-part wedge mechanism to assess direct sliding resistance (e.g., Schmertmann et al., 1987).

4. From the viewpoint of construction, placement of reinforcement at close spacing in segmental walls is easy and practical. The spacing is dictated by the height of modular facing blocks (typically, minimum height is 20 cm). Walls with short reinforcement are sometimes needed, especially when back space is limited (e.g., repair of a failed slope). Hence, the design implications may indeed be significant.

It must be stated that the aforementioned design implications are restricted to closely spaced reinforcement. However, how far layers can be spaced and still be considered "closely spaced" so that an internal active wedge will not develop is not clear at the present time. More studies are needed to identify this maximum spacing. For example, Bathurst and Benjamin (1990) observed an internal slip surface when the geogrid spacing was 75 cm. These tests were conducted with reinforcement that immediately mobilizes significant tensile resistance with strain (i.e., the facing cannot move outward without first activating the geogrid's resistance). It should be noted that geotextiles and some geogrids have an S-shaped load-elongation curve, indicating there will be little resistance mobilized during initial straining. The effects of this initial "softness" on the formation of active wedge, as assumed in current design, are not clear and more studies are therefore needed on such materials. Moreover, the design implications ignore wall face deformations. This performance aspect needs further study, especially for low quality backfill. Finally, this research work does not provide information about the tensile forces mobilized in the geogrid, an important factor in selecting a reinforcement and in ensuring that breakage and creep do not occur. Numerous field tests, however, indicate that strength selected based on Rankine's analysis is quite conservative.

ACKNOWLEDGEMENT

This research project was partially funded by Tensar Earth Technologies, Inc. This support is gratefully acknowledged.

REFERENCES

1) Bathurst, R. J. and Benjamin, D. J. (1990): "Failure of a geogrid reinforced soil wall," Transportation Research Record, Vol. 1228, pp. 109–116.
2) Jewell, R. A. (1990): "Strength and deformation in reinforced soil design," Proceedings of 4th International Conference on Geotextiles, Geomembranes and Related Products, The Hague, Netherlands, Balkema, editor G. Den Hoedt, Vol. 3, pp. 913–946.
3) Leshchinsky, D. and Perry, E. B. (1989): "On the design of geosynthetic-reinforced walls," Geotextiles and Geomembranes, Vol. 8, No. 4, pp. 311–323.
4) McGown, A., Andrawes, K., Yeo, K. and Dubois, D. (1984): "The load-strain-time behavior of Tensar geogrids," Symposium on Polymer Grid Reinforcement in Civil Engineering, Paper No. 1.2, London.
5) Schmertmann, G. R., Chourey-Curtis, V. E., Johnson, R. D. and Bonaparte, R. (1987): "Design charts for geogrid-reinforced soil slopes." Proceeding of Geosynthetics '87 Conference, Industrial Fabrics Association International, Vol. 1, pp. 108–120.